

RESEARCH

Open Access



Cross-species transcriptome-wide meta-analysis of anterior cruciate ligament rupture

Livia Beccacece¹, Stefano Pallotti¹, Yiyun Li¹, Jie Huang², Leonardo Pasotti³ and Valerio Napolioni^{1*}

Abstract

Background The Anterior Cruciate Ligament (ACL) plays a critical role in maintaining the musculoskeletal stability of the knee. Its injury has been linked to an increased risk of developing osteoarthritis. This study aims to identify cross-species responses to ACL rupture providing insights on its molecular basis. We analyzed five publicly available transcriptomic datasets from *Homo sapiens*, *Mus musculus*, *Canis lupus familiaris*, and *Oryctolagus cuniculus*. Differential gene expression analysis was performed for each dataset, producing a genome-wide transcriptional signature of fold-change significance for individual genes. Stouffer's method was used to integrate the results, identifying genes significantly deregulated across all species. Additionally, gene-set enrichment analysis revealed pathways that were consistently upregulated or downregulated.

Results A positive correlation in expression was observed between human and the other three species ($r^2 = 0.177 - 0.305$, $p\text{-value} \leq 2.7 \times 10^{-113}$), identifying 210 genes as the most consistently up- and down-regulated in response to ACL rupture ($p\text{-adjusted} \leq 1.27 \times 10^{-23}$). These genes are primarily involved in cellular mitosis, collagen pathways, and cartilage development. Furthermore, 60 pathways were found to be significantly up- or down-regulated across all species ($p\text{-adjusted} \leq 4.57 \times 10^{-4}$). Among these, the upregulation of inhibition of bone mineralization ($p\text{-adjusted} \leq 2.99 \times 10^{-6}$) aligns with previous findings on the reduction of subchondral bone mineral density following ACL rupture.

Conclusions This study highlights that distinct species exhibit common molecular responses to ACL rupture, underscoring the value of mice, dogs, and rabbits as potential translational model organisms for ACL rupture research. Furthermore, the identified genes and pathways highlight the molecular mechanisms underlying ACL rupture.

Keywords Anterior cruciate ligament rupture, Transcriptomics, Cross-species meta-analysis, Translational genomics

*Correspondence:

Valerio Napolioni
valerio.napolioni@unicam.it

¹Genomic And Molecular Epidemiology (GAME) Lab, School of Biosciences and Veterinary Medicine, University of Camerino, Via Gentile da Varano III, Camerino 62032, Italy

²School of Public Health and Emergency Medicine, Southern University of Science and Technology, Shenzhen, China

³Complex Orthopedics and Traumatology Unit, AST Macerata, Camerino Hospital, Camerino, Italy



© The Author(s) 2025. **Open Access** This article is licensed under a Creative Commons Attribution-NonCommercial-NoDerivatives 4.0 International License, which permits any non-commercial use, sharing, distribution and reproduction in any medium or format, as long as you give appropriate credit to the original author(s) and the source, provide a link to the Creative Commons licence, and indicate if you modified the licensed material. You do not have permission under this licence to share adapted material derived from this article or parts of it. The images or other third party material in this article are included in the article's Creative Commons licence, unless indicated otherwise in a credit line to the material. If material is not included in the article's Creative Commons licence and your intended use is not permitted by statutory regulation or exceeds the permitted use, you will need to obtain permission directly from the copyright holder. To view a copy of this licence, visit <http://creativecommons.org/licenses/by-nc-nd/4.0/>.

Background

The anterior cruciate ligament (ACL) plays a crucial role in knee kinematics and rotation by controlling the anterior movement of the tibia and inhibiting extreme rotations [1]. ACL injuries impact musculoskeletal and joint stability and are associated with an increased risk of developing post-traumatic osteoarthritis (PTOA) [2], an inflammatory chronic disease characterized by damage to articular cartilage, inflammation of the synovium, and loss of subchondral bone [3, 4]. ACL disruption often occurs in athletes, with a higher incidence in females, influenced by various risk factors such as ligament thickness, quadriceps angle and quadriceps-hamstring mass ratio, geometry of the intercondylar notch, and hormonal influences [5]. Additionally, a high body mass index and genetic factors can exacerbate the etiopathogenesis of non-contact ligament injuries [6, 7]. Translational studies have proven effective in exploring the molecular basis of human diseases [8]. Notably, species like dogs provide a more accurate model for human disorders, as they often exhibit pathophysiological and clinical features similar to those in humans [9]. Research has been conducted not only on humans [10] but also on animal models such as mice [11], rabbits [12], and dogs [13] to uncover the mechanisms underlying ACL injury. However, a study that includes both human and animal model samples has yet to be conducted. In light of this, we performed a cross-species meta-analysis that includes humans, dogs (*Canis lupus familiaris*), rabbits (*Oryctolagus cuniculus*), and mice (*Mus musculus*), focusing on transcriptome-wide data to determine whether ACL disruption leads to alterations in biological processes conserved across species.

Methods

Data retrieving and processing

We conducted a search of transcriptome-wide datasets that met our inclusion criteria of anterior cruciate ligament rupture and sampled tissues (ACL and/or synovium) on the BioProject database [14], hosted by the National Center for Biotechnology Information (NCBI). We selected six publicly available transcriptome-wide datasets belonging to four species: *Homo sapiens*,

Mus musculus, *Canis lupus familiaris*, and *Oryctolagus cuniculus* (Table 1) [11–13, 15, 16]. We retrieved raw sequence data (FASTQ files) from the Sequence Read Archive (SRA) database using SRA Toolkit version 2.11.0 [14]. Quality control was performed using FastQC version 0.11.9 [17], and poor-quality reads were trimmed using Trimmomatic version 0.39 [18], which was also used to remove sequencing adapters. A human dataset (PRJNA879078) [15] was excluded from the following analyses due to relevant differences in sequencing read length. Sequence reads were aligned to their respective reference genomes (human genome version GRCh38.113, mouse genome version GRCm39.113, dog genome version ROS_Cfam_1.0.113, and rabbit genome version OryCun2.0.113) using the STAR aligner tool v.2.7.10a [19]. The aligned reads were then processed using featureCounts v.2.0.8 [20] to obtain matrices of gene counts for each sample.

Differential gene expression analysis, Pearson correlation analysis, Stouffer integration, and pathway enrichment analysis were executed on R statistical software version 4.4.3. All graphs were generated through ggplot2 R package version 3.5.1 [21].

Differential gene expression analysis

Differential gene expression (DEG) analysis was conducted to evaluate the transcriptome-wide responses to ACL rupture. The analysis utilized gene counts through the DESeq2 R package version 1.46.0 [22], applying an “injured vs. control” design for a total of 19 DEG contrasts across all datasets. To eliminate bias from differing tissue samples, four rabbit samples from the medial collateral ligament [12] and 24 mouse samples from contralateral knee joints [11] were excluded from both the DEG and subsequent analyses.

A transcriptome-wide signature of fold-change significance was created for each contrast of the datasets using the formula $-\log_{10}(p\text{-value}) \times \text{sign}(\log(\text{fold-change}))$. This formula assigned positive numeric values to significantly up-regulated genes and negative ones to significantly down-regulated genes, and the extent of this value is proportional to expression change significance.

Table 1 Transcriptomics datasets included in the study

Accession number	Species	Samples	Assay type	Tissue	Reference
PRJNA694471	<i>Homo sapiens</i>	6	RNA-seq	ACL	/
PRJNA879078*	<i>Homo sapiens</i>	12	RNA-seq	Synovial tissue	[15]
PRJNA448594	<i>Mus musculus</i>	100	RNA-seq	Femoral and tibial joint regions	[16]
PRJNA1134075	<i>Mus musculus</i>	61	RNA-seq	Synovial tissue	[11]
PRJEB43144	<i>Canis lupus familiaris</i>	16	RNA-seq	ACL, Synovial tissue	[13]
PRJNA751479	<i>Oryctolagus cuniculus</i>	8	RNA-seq	ACL, Medial collateral ligament	[12]

*The human dataset with accession number PRJNA879078 was excluded due to differences in reads length among samples (6 samples with sequence length of 100 bp and 6 samples with sequence length of 15–45 bp)

Phylogenetic gene conversion

To facilitate the comparison of expression changes among different species, a phylogenetic ortholog conversion of signature genes to human genes has been implemented for each animal species included in this study. Ortholog prediction was performed using the DRSC Integrative Ortholog Prediction (DIOPT) tool version 9 [23] for *M. musculus*, while we used the orthogene R package version 1.12.0 [24] via the gprofiler method for

Table 2 Number of up- and down-regulated genes in each species

Species	Contrast identifier*	Up-regulated genes**	Down-regulated genes**
<i>H. sapiens</i>	Hs_acl	1,787	1,871
<i>M. musculus</i>	Mm_C57BL/6_1d	0	0
<i>M. musculus</i>	Mm_C57BL/6_1w	0	0
<i>M. musculus</i>	Mm_C57BL/6_2w	1,347	1,068
<i>M. musculus</i>	Mm_MRL/MpJ_1d	723	480
<i>M. musculus</i>	Mm_MRL/MpJ_1w	3	185
<i>M. musculus</i>	Mm_MRL/MpJ_2w	264	1
<i>M. musculus</i>	Mm_STR/ort_1d	857	678
<i>M. musculus</i>	Mm_STR/ort_1w	1,623	1,090
<i>M. musculus</i>	Mm_STR/ort_2w	1,506	704
<i>M. musculus</i>	Mm_syn_F_1W	4,819	4,864
<i>M. musculus</i>	Mm_syn_F_4W	1,455	738
<i>M. musculus</i>	Mm_syn_M_1W	3,117	1,713
<i>M. musculus</i>	Mm_syn_M_4W	2,189	763
<i>C. lupus familiaris</i>	Clf_acl_lab	189	192
<i>C. lupus familiaris</i>	Clf_acl_gold	259	463
<i>C. lupus familiaris</i>	Clf_syn_lab	794	441
<i>C. lupus familiaris</i>	Clf_syn_gold	827	640
<i>O. cuniculus</i>	Oc_acl	290	187

*Legend of identifiers: Hs_acl=*H. sapiens*, anterior cruciate ligament (PRJNA694471); Mm_C57BL/6_1d=*M. musculus*, C57BL/6 mouse strain, femoral and tibial joint regions, 1 day after injury (PRJNA448594); Mm_C57BL/6_1w=*M. musculus*, C57BL/6 mouse strain, femoral and tibial joint regions, 1 week after injury (PRJNA448594); Mm_C57BL/6_2w=*M. musculus*, C57BL/6 mouse strain, femoral and tibial joint regions, 2 weeks after injury (PRJNA448594); Mm_MRL/MpJ_1d=*M. musculus*, MRL/MpJ mouse strain, femoral and tibial joint regions, 1 day after injury (PRJNA448594); Mm_MRL/MpJ_1w=*M. musculus*, MRL/MpJ mouse strain, femoral and tibial joint regions, 1 week after injury (PRJNA448594); Mm_MRL/MpJ_2w=*M. musculus*, MRL/MpJ mouse strain, femoral and tibial joint regions, 2 weeks after injury (PRJNA448594); Mm_STR/ort_1d=*M. musculus*, STR/ort mouse strain, femoral and tibial joint regions, 1 day after injury (PRJNA448594); Mm_STR/ort_1w=*M. musculus*, STR/ort mouse strain, femoral and tibial joint regions, 1 week after injury (PRJNA448594); Mm_STR/ort_2w=*M. musculus*, STR/ort mouse strain, femoral and tibial joint regions, 2 weeks after injury (PRJNA448594); Mm_syn_F_1W=*M. musculus*, synovial tissue, female mouse, 1 week after injury (PRJNA1134075); Mm_syn_F_4W=*M. musculus*, synovial tissue, female mouse, 4 weeks after injury (PRJNA1134075); Mm_syn_M_1W=*M. musculus*, synovial tissue, male mouse, 1 week after injury (PRJNA1134075); Mm_syn_M_4W=*M. musculus*, synovial tissue, male mouse, 4 week after injury (PRJNA1134075); Clf_acl_lab=*C. lupus familiaris*, anterior cruciate ligament, labrador retriever (PRJEB43144); Clf_acl_gold=*C. lupus familiaris*, anterior cruciate ligament, golden retriever (PRJEB43144); Clf_syn_lab=*C. lupus familiaris*, synovial tissue, labrador retriever (PRJEB43144); Clf_syn_gold=*C. lupus familiaris*, synovial tissue, golden retriever (PRJEB43144); Oc_acl=*O. cuniculus*, anterior cruciate ligament (PRJNA751479)

***p*-adjusted < 0.05, Benjamini-Hochberg adjustment

the other species. The resulting signature matrix, which contains 19 contrasts and the human gene identifiers, was used for subsequent analyses.

Cross-species meta-analysis

To assess the similarities in transcriptional responses to ACL rupture across distinct species, we performed Pearson correlation followed by cross-species integration using the Stouffer method, as implemented in the corto R package v.1.2.4. To identify the most significantly deregulated genes across species, *p*-values were calculated using Z-scores [25].

For the pathway enrichment analysis, gene sets were retrieved from Gene Ontology [26, 27], KEGG [28, 29], and WikiPathways [30] using the Molecular Signature Database (MSigDB) [31], accessed via the msigdb R package version 7.5.1 [32]. Gene Set Enrichment Analysis [33] was performed for each contrast of the signature matrix by utilizing the fgsea R package version 1.32.2 [34] to identify the up- and down-regulated pathways. The normalized enrichment score (NES) resulting from the analysis was then integrated using the Stouffer method, and Z-scores were converted to *p*-values to determine the most significantly up- and down-regulated pathways across species; this was achieved through the corto R package [25]. An additional pathway enrichment analysis was done using clusterProfiler R package version 4.4.4 [35].

Results

Gene expression changes

All species exhibit numerous significantly up- and down-regulated genes (*p*-adjusted < 0.05, FDR adjustment) in response to ACL injury (Table 2). The results of the differential gene expression analysis for each tested contrast are available in Supplementary File 1.

Cross-species correlation

A Pearson correlation was conducted to assess whether ACL rupture involves similar molecular mechanisms across different species. Overall, there is evidence of intra- and inter-species correlations (Fig. 1), with a predominance of positive associations. The highest positive values are observed in intra-species comparisons (*M. musculus* and *C. lupus familiaris*). However, it is interesting to note that *M. musculus* exhibits negative correlations when considering distinct experimental conditions (mouse strains and timing after the injury), which may have an opposite effect on genes deregulation following ACL disruption.

In addition to intra-species correlations, the analysis revealed that the injury elicits correlated responses between humans and the other three species included in the study. The strongest inter-species correlation was

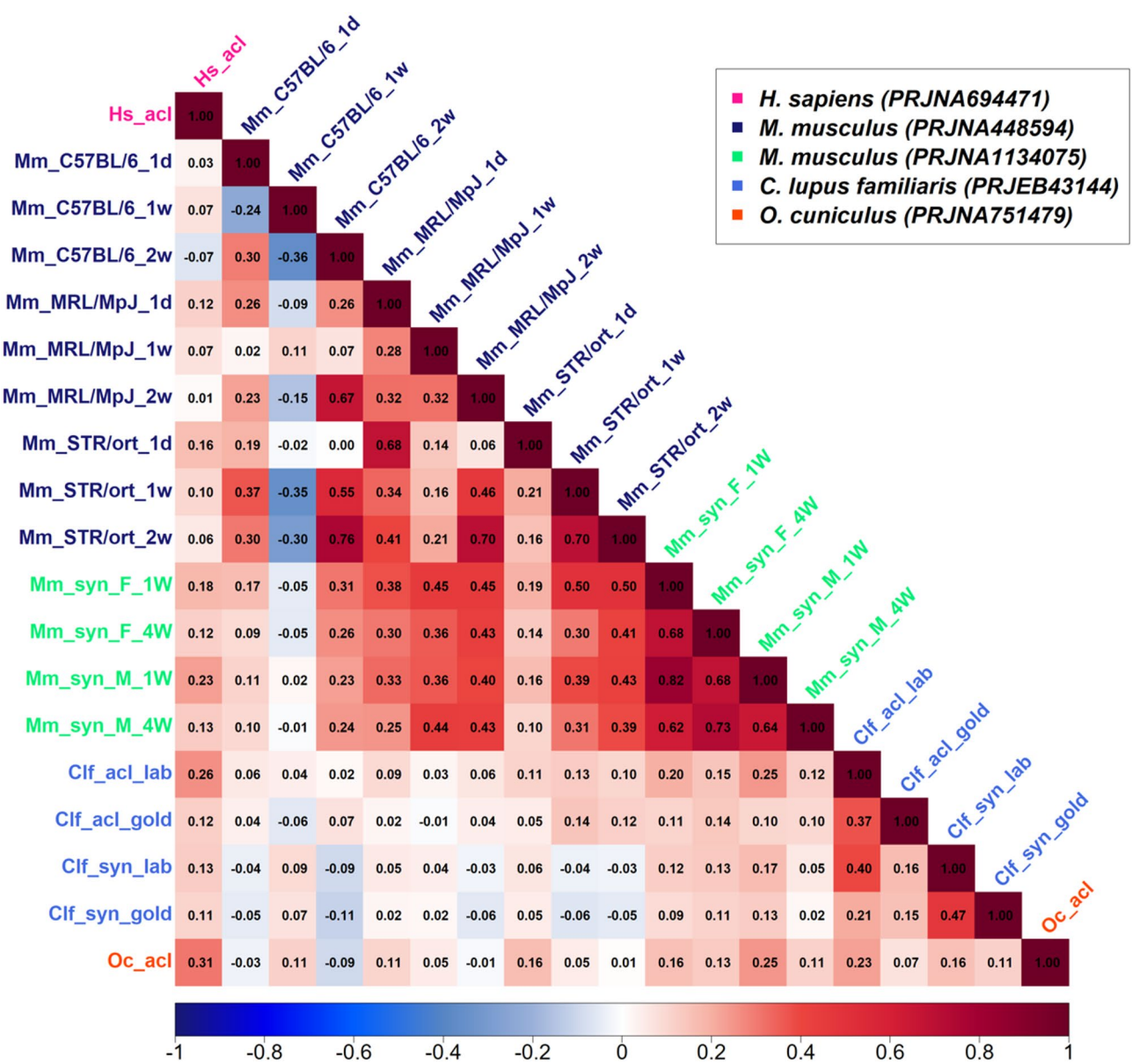


Fig. 1 Correlation plot showing the correlation between the 19 contrasts included in the meta-analysis. Colors of boxes range from blues (negative correlation) to reds (positive correlation). Inside each box there is the correlation coefficient (r^2). Legend of identifiers can be found in the notes to Table 2

observed between *H. sapiens* and *O. cuniculus*, which is extremely significant ($r^2 = 0.305$, $p\text{-value} = 6.24 \times 10^{-295}$); furthermore, *H. sapiens* shows significant correlations even with *M. musculus* ($r^2 = 0.177$, $p\text{-value} = 2.7 \times 10^{-113}$) and *C. lupus familiaris* ($r^2 = 0.260$, $p\text{-value} = 4.15 \times 10^{-226}$). As shown in Fig. 2, the positive correlation among humans and the other species is influenced by genes that are both up- and down-regulated. Additionally, there is evidence that the dysregulation of genes in dogs, mice, and rabbits correlates with one another.

Cross-species response to ACLR

Once it was established that ACL rupture stimulates overlapping gene expression alterations in the four species, the focus shifted to identifying the genes that trigger the conserved response and are thereby deregulated in all species. We conducted a Stouffer integration on the signature matrix to assign equal importance to all species, despite their uneven representation due to the differing number of analyzed contrasts for each species. Overall, 12,336 genes are differentially expressed among the four species included in the study, with 383 genes identified as significantly dysregulated (Fig. 3). Among these, 173 genes, highlighted in yellow and

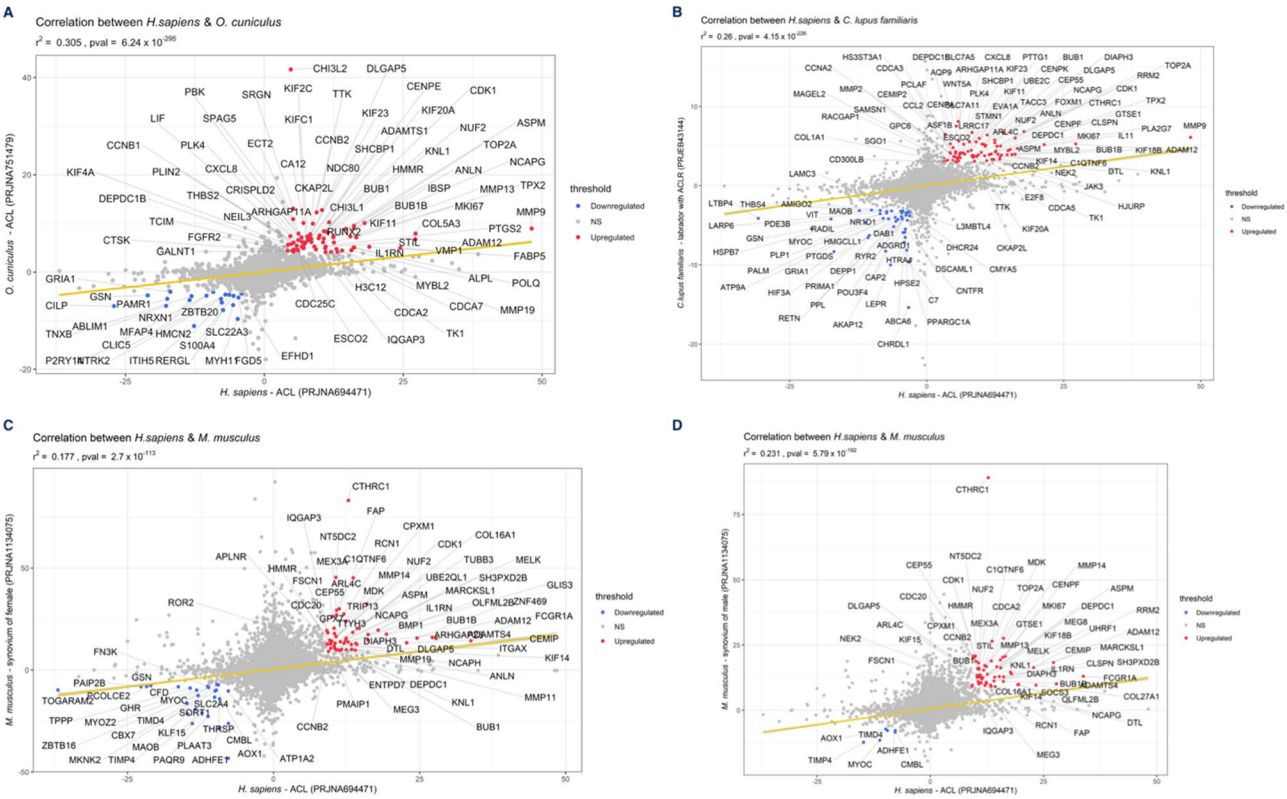


Fig. 2 (A) Scatterplot displaying the correlation between *H. sapiens* and *O. cuniculus*; the highlighted genes are the most significantly up- (red dots) and down-regulated (blue dots) genes in both species ($p\text{-value} \leq 10^{-5}$) and drive the correlation. (B) Scatterplot displaying the correlation between *H. sapiens* and *C. lupus familiaris*, specifically labrador retriever with ACL as sampled tissue; the highlighted genes are the most significantly up- (red dots) and down-regulated (blue dots) genes in both species ($p\text{-value} \leq 0.001$) and drive the correlation. (C) Scatterplot displaying the correlation between *H. sapiens* and *M. musculus*, specifically female mouse with synovium sampled 1 week after the injury; the highlighted genes are the most significantly up- (red dots) and down-regulated (blue dots) genes in both species ($p\text{-value} \leq 0.001$) and drive the correlation. (D) Scatterplot displaying the correlation between *H. sapiens* and *M. musculus*, specifically male mouse with synovium sampled 1 week after the injury; the highlighted genes are the most significantly up- (red dots) and down-regulated (blue dots) genes in both species ($p\text{-value} \leq 0.001$) and drive the correlation

green in Fig. 3 and listed in Supplementary Table S2A, are significantly up- and down-regulated across species (Stouffer integrated Z-scores $>|10|$, corresponding to a $p\text{-value}$ of 1.52×10^{-23}), though there are considerable differences across species (standard deviation $>|10|$), suggesting that the deregulation is pronounced in only a few contrasts. In contrast, 210 genes are significantly deregulated (Stouffer integrated Z-scores $>|10|$), but they exhibit lower fluctuations across species (standard deviation $<|10|$), indicating that these genes represent the core of a conserved molecular response to ACL rupture (blue and red dots in Fig. 3, Supplementary Table S2B). From this list, we extracted the top 10% of both up- and down-regulated genes (Table 3; Stouffer integrated Z-scores $>|10|$, $p\text{-adjusted}$ of 2.60×10^{-47} , FDR adjustment).

We executed a pathway enrichment analysis, including the top 210 genes, to determine the metabolisms in which they are implicated. Overall, 3,394 pathways are enriched by these genes, of which 222 reach the significance threshold ($p\text{-adjusted} \leq 0.05$, FDR adjustment). Figure 4 displays the most significant pathways ($p\text{-adjusted} \leq$

1.10×10^{-5} , FDR adjustment), indicating that these genes are mainly involved in cellular mitosis, collagen pathways, and cartilage development.

Gene set enrichment analysis

Gene set enrichment analysis was carried out to detect the biological mechanisms most affected by ACL rupture. We integrated the Normalized Enrichment Score (NES) among all datasets' contrasts to pinpoint the more consistently up- and down-regulated pathways across species. We identified 4,759 pathways that are significantly dysregulated across species (integrated $p\text{-adjusted} \leq 0.05$, FDR adjustment). Figure 5 shows the most significantly up- and down-regulated pathways.

As shown in Fig. 5, ACL rupture impacts various biological processes. For example, the p53 signaling pathway (KEGG, $p\text{-adjusted} = 7.13 \times 10^{-8}$, FDR adjustment) and negative regulation of bone mineralization (GOBP, $p\text{-adjusted} = 2.99 \times 10^{-6}$, FDR adjustment) are upregulated, whereas the long-chain fatty acid biosynthetic process (GOBP, $p\text{-adjusted} = 4.21 \times 10^{-6}$, FDR adjustment)

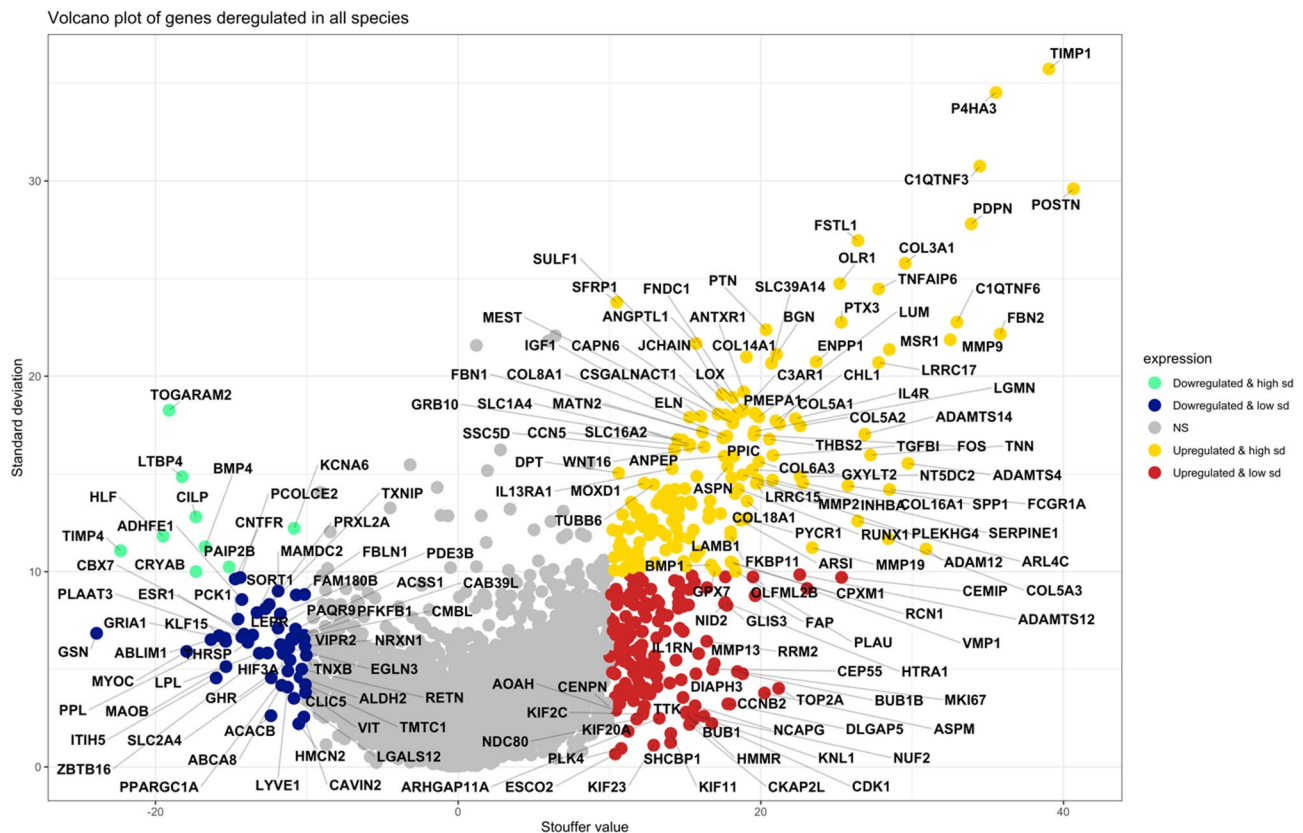


Fig. 3 Plot displaying the cross-species integrated response to anterior cruciate ligament rupture. The Stouffer value on x-axis indicates the integrated signature value, obtained through the integration of signature across the datasets by utilizing Stouffer method. On the y-axis there is the standard deviation of the signature across the datasets. In red and yellow there are the genes with highest positive integrated signature, which are upregulated across species; in blue and green there are the genes with highest negative integrated signature, which are downregulated across species. The dots in yellow and green have the highest fluctuations across the datasets

and lipid metabolism pathway are downregulated (WP, p -adjusted = 3.94×10^{-7} , FDR adjustment).

Discussion

Despite differences in the anatomy of the knee and anterior cruciate ligament between humans and other animal species [36], our study identified convergent transcriptional alterations across species induced by ACL disruption. In many studies that use animals as models for human ACL rupture (such as mice and rabbits), the ligament is surgically transected [37]. However, ACL disruption shows some similarities between humans and dogs [38]; indeed, both species are more prone to a spontaneous onset of the injury and have an increased risk of developing post-traumatic osteoarthritis [38].

Overall, we identified a core group of genes demonstrating a cross-species conserved response to ACL rupture. These genes are involved in various distinct metabolic processes, several of which are associated with mitosis and its regulation, collagen binding and organization, the breakdown of the extracellular matrix, the development of connective tissue and cartilage, and

ossification. Notably, the enrichment of pathways related to mitosis may align with previous findings that observed an increase in fibrocyte proliferation following ACL disruption in humans, along with heightened angiogenesis in both the synovium and ACL [39].

Some of the top 10% differentially expressed genes in our samples (Table 3), encoding enzymes involved in proteolytic activity, autophagy induction, regulation of the mitotic process, transcription regulation, and extracellular matrix stabilization, have previously been identified as dysregulated after anterior cruciate ligament disruption and osteoarthritis. Specifically, the upregulation of *VMP1* and *TOP2A*, along with the downregulation of *GSN*, has already been observed in porcine synovium following ACL transection [40]. Similarly, variants in *OLFML2B*, a gene upregulated in our samples after ACL rupture, have been linked to an increased risk of non-contact ACL rupture in humans [41].

Several genes upregulated in our sample have also been linked to osteoarthritis in various species. *ADAMTS12*, which is essential for tendon maintenance, has been shown to be involved in the progression of osteoarthritis

Table 3 Table showing the top 10% dysregulated genes across species

Gene	Stouffer value	Standard deviation	p-adjusted*
<i>CEMIP</i>	25.3357199	9.71226471	2.71×10^{-139}
<i>VMP1</i>	23.057659	9.14444267	8.63×10^{-116}
<i>ADAMTS12</i>	22.5712722	9.84778032	4.36×10^{-111}
<i>TOP2A</i>	21.1795111	4.02365932	6.20×10^{-98}
<i>ASPM</i>	20.2395895	3.78516438	1.54×10^{-89}
<i>FAP</i>	19.6239809	8.77073799	2.89×10^{-84}
<i>OLFML2B</i>	19.4848792	9.73187037	3.87×10^{-83}
<i>BUB1B</i>	18.7945286	4.77117528	1.95×10^{-77}
<i>MKI67</i>	18.4529349	4.88371517	1.04×10^{-74}
<i>CCNB2</i>	17.9602446	3.21936435	7.62×10^{-71}
<i>PCK1</i>	-14.540771	7.56899307	2.60×10^{-47}
<i>CNTFR</i>	-14.733198	9.62428079	1.73×10^{-48}
<i>MAOB</i>	-15.34104	5.13867285	2.37×10^{-52}
<i>PPL</i>	-15.360225	6.42863234	1.82×10^{-52}
<i>GRIA1</i>	-15.409135	6.59162292	8.78×10^{-53}
<i>KLF15</i>	-15.80532	6.71802791	2.22×10^{-55}
<i>ITIH5</i>	-15.991118	4.55626263	1.24×10^{-56}
<i>ABLIM1</i>	-16.332788	6.51557864	5.27×10^{-59}
<i>MYOC</i>	-17.9381	5.91536112	1.04×10^{-70}
<i>GSN</i>	-23.891389	6.84437937	3.95×10^{-124}

*The p-adjusted is indicative of integrated significance; it was calculated by converting the Z-scores into p-values that were corrected though FDR adjustment

following ACL disruption in both humans [42] and rats [43]. Similarly, *ASPM*, a gene within the cluster of tendon stem/progenitor cells and anterior cruciate ligament fibroblasts, is known to play a role in the progression of knee osteoarthritis progression [44].

Additionally, *BUB1B* and *CCNB2* have been found to be differentially expressed in osteoarthritic cartilage compared to normal cartilage, potentially contributing to the inflammatory response, negatively regulating cell proliferation, and promoting the ossification characteristic of the disease [45]. Furthermore, the overexpression of *CEMIP*, which encodes cell migration-inducing hyaluronidase 1, has been linked to the pathogenesis of osteoarthritis [46]. The *CEMIP* enzyme primarily participates in the trafficking and degradation of hyaluronic acid (HA) [47] by producing intermediate-sized HA (int-HA) and low-molecular-weight HA (LMW-HA) fragments that are involved in inflammation [47, 48]. Its overexpression in chondrocytes and synovial fibroblasts has been associated with articular cartilage degeneration in osteoarthritis [46, 49, 50], mediating fibrosis in chondrocytes [51] and promoting the inflammatory process due to increased levels of LMW-HA in synovial fluid [49, 50]. Downregulation of *ITIH5* in synovial tissues during osteoarthritis has also been reported, which may contribute to the histological alterations observed in the synovium during the condition [52], while a deficiency of the *KLF15* gene exacerbates osteoarthritis, resulting in

significant cartilage degradation as evidenced in KLF15-KO-DMM mice [53]. Finally, *FAP* has been identified as a critical pathogenic factor in osteoarthritis due to its role in cartilage matrix degradation [54]. Some genes downregulated in our sample may be indirectly related to ACL rupture and osteoarthritis due to their involvement in the physiology of various connective tissues. This includes *CNTFR*, *GRIA1*, and *ABLIM1*, which are essential for bone cell biology [55–57]. *CNTFR* is essential for osteoblast function, playing a key role in the normal remodeling of trabecular bone and the proper growth of both cortical and longitudinal bone [55]. Downregulation of this gene has already been observed in cartilage following AO lesions in human [58] and rat [59]. Inhibition of *GRIA1*, for instance, promotes osteoporosis and may contribute to fractures by suppressing the osteogenic differentiation of bone marrow mesenchymal stem cells [56]. Meanwhile, *ABLIM1* plays an important role in the pathogenesis of ossification of the posterior longitudinal ligament, a condition marked by ectopic bone formation [57]. Additionally, *ABLIM1* may have muscle-specific functions, with abnormal splicing of the gene potentially linked to muscle symptoms in Myotonic Dystrophy Type 1 [60]. The downregulation of *MYOC*, which regulates muscle hypertrophy and atrophy pathways, may also contribute to ACL rupture. Notably, *MYOC* is the major protein enriched in the ACL and patellar tendon in males compared to females, which may help explain the higher incidence of ACL rupture observed in females [61]. Lastly, dysregulation of *PPL* has been noted in the cardinal ligament of women with pelvic organ prolapse, suggesting a role for this gene in maintaining ligament tissue physiology [62].

We found that ACL disruption affects many pathways involved in several biological processes. The deregulation of some of these pathways may play a role in the pathogenesis of post-traumatic osteoarthritis following anterior cruciate ligament rupture. As mentioned, cartilage degeneration is a primary feature of osteoarthritis, and the upregulation of the p53 signaling pathway induced by ACL injury may contribute to PTOA pathogenesis. P53, a well-known multifunctional transcription factor, is involved in DNA repair, cell cycle arrest, and even apoptosis in response to cellular stress [63]. Previous findings have shown that p53 is overexpressed in the cartilage of individuals with knee osteoarthritis, worsening the pathological state [64] and inducing chondrocyte senescence, which leads to cell accumulation, autophagy, apoptosis, and cartilage damage [65, 66]. ACL injury leads to the upregulation of inhibition of bone mineralization across all species, suggesting involvement in PTOA pathogenesis, which is characterized by subchondral bone degeneration and cartilage loss [3, 4]. A previous follow-up study detected lower mineral density of the proximal

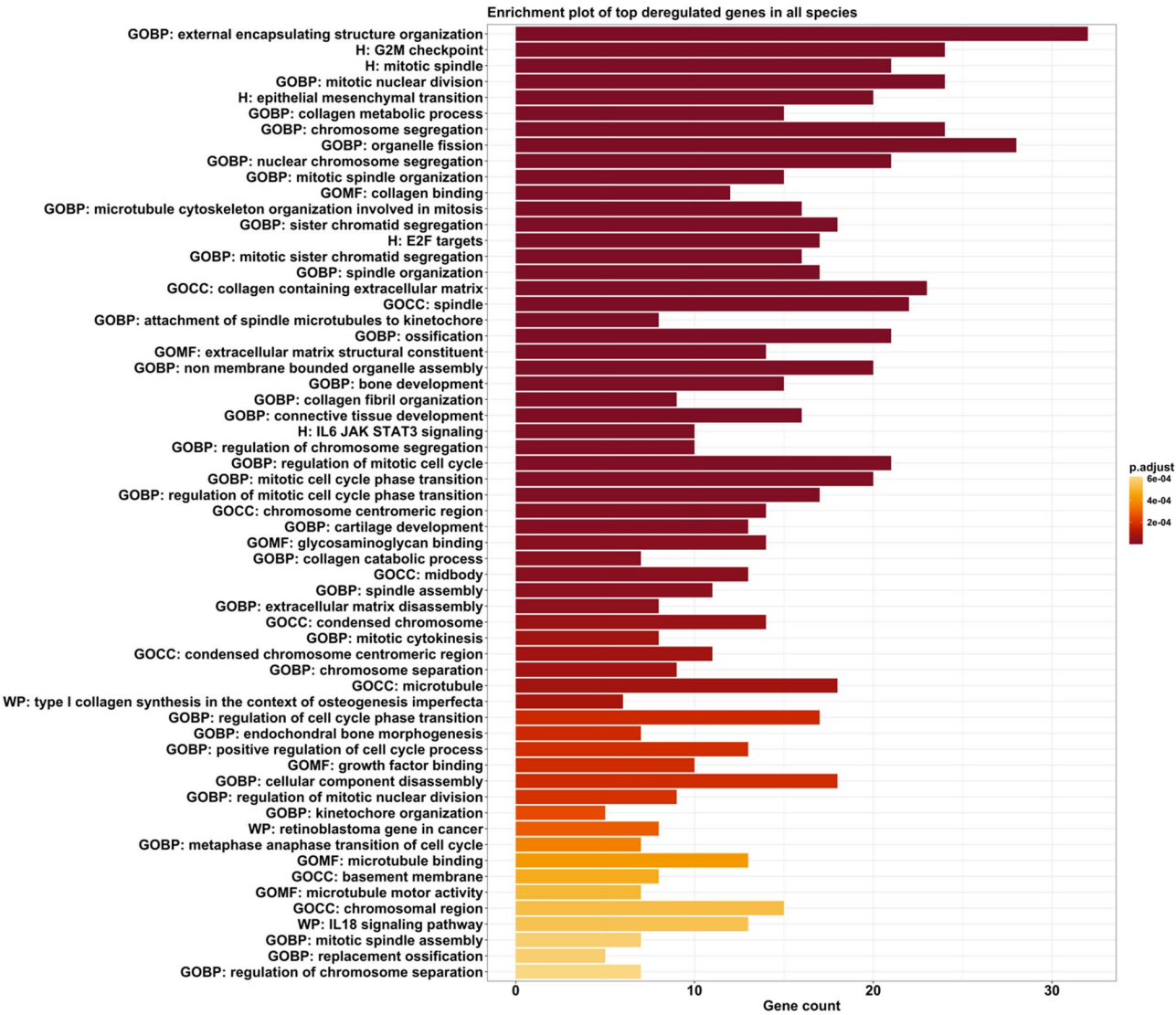


Fig. 4 Most significant pathways enriched by the most significantly deregulated genes across species. All pathways display p -adjusted $\leq 6 \times 10^{-4}$ (FDR adjustment)

tibia compared to the contralateral knee and fluctuations in the mineralization of the distal femur during the two years after ACL injury [67]. Moreover, femur entheses of the anterior cruciate ligament is affected by bone loss in both females [68] and males [69]. Similarly, bone resorption has been observed in young mice [70]. Thus, downregulation of this pathway could play a role in PTOA development, as it has been proposed that bone remodeling, demineralization, and reduced density can contribute to the initiation and progression of osteoarthritis [71]. Lipid metabolism and long-chain fatty acids biosynthesis pathways are significantly downregulated across species. The downregulation of lipid metabolism was already pinpointed in porcine synovium following ACL transection [40], and lipid metabolism is likely related to osteoarthritis [72]. Alterations of lipid composition in bone marrow

(higher levels of unsaturated lipids) have been detected in patients with ACL damage and those with knee osteoarthritis [73], likely contributing to bone degeneration typical of osteoarthritis. However, how the downregulation of lipid metabolism contributes to osteoarthritis still needs more investigation. In contrast, the role of long-chain fatty acids on osteoarthritis has already been ascertained. Long-chain polyunsaturated fatty acids (LCPUFAs) have a different effect on chondrocytes depending on the fatty acid molecule; specifically, n-3 LCPUFAs play a protective role on cartilage, while n-6 LCPUFAs block chondrocytes differentiation, determining cartilage degeneration and osteoarthritis development [74]. These fatty acids modulate osteogenesis, by promoting the differentiation of mesenchymal stem cells into adipocytes or osteoblasts depending on levels of these acids [75] and, at same

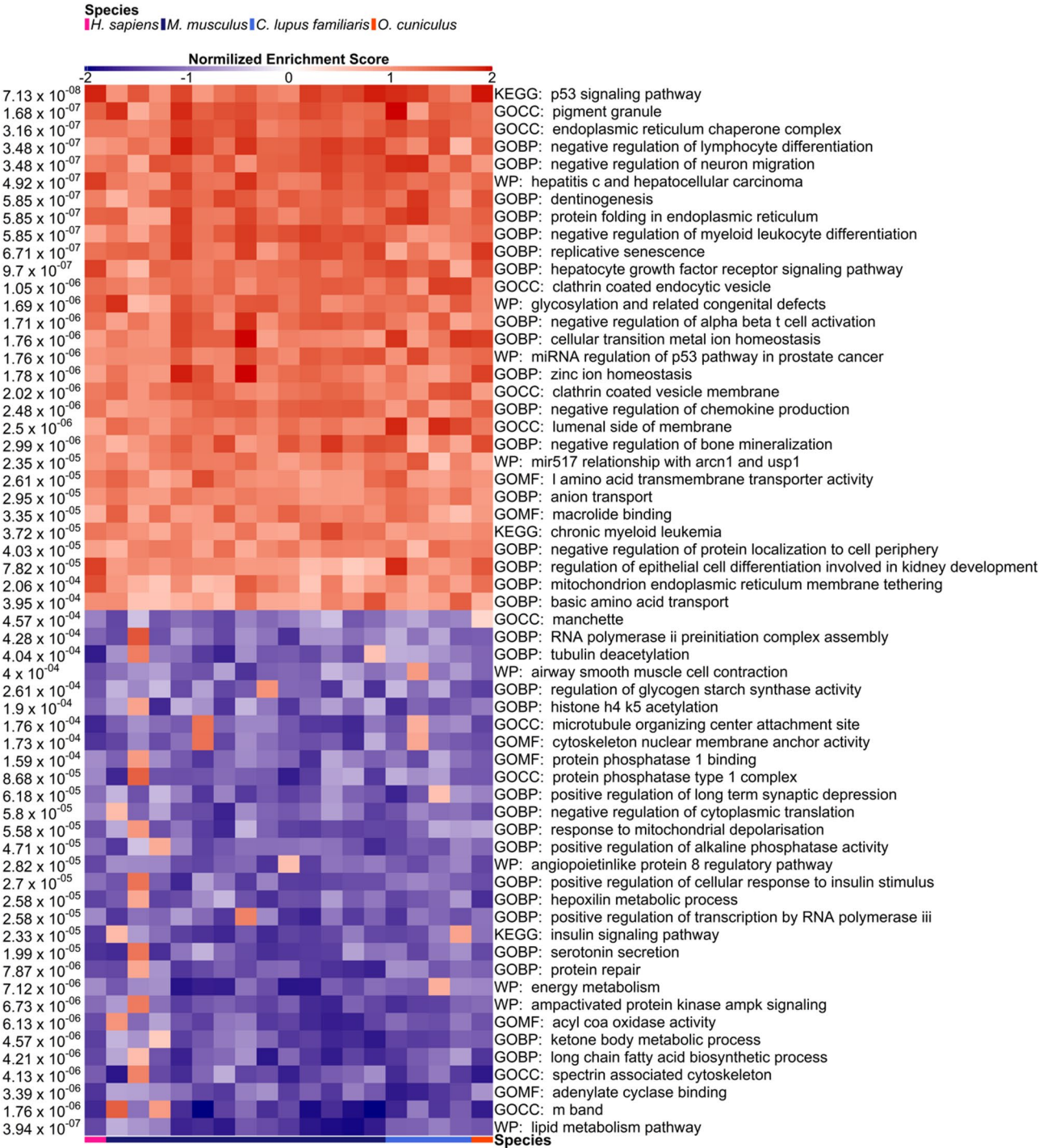


Fig. 5 Heatmap displaying the 60 most significantly up- and down-regulated pathways across species. Blue and red color scales are proportional to the calculated Normalized Enrichment Score of the pathway. The top bar indicates the species of the contrasts through a distinct color. On the left side of the figure, the *p*-adjusted is indicative of the integrated significance of enrichment of pathway calculated across species and the correction for multiple testing was executed through Benjamini-Hochberg method

time, induce osteoclastogenesis in bone marrow-derived monocytes/macrophages precursor cells whereas inhibit it in bone marrow cells [76]. It is possible that alterations in the biosynthesis of long-chain fatty acids could contribute to osteoarthritis pathogenesis.

Limitations

This study offers a comprehensive overview of gene upregulation and downregulation following ACL injury across four species. However, further research is needed to validate our preliminary findings, and several limitations should be acknowledged. We conducted the search of publicly available datasets on BioProject up until 15 November 2024 and the datasets published later were excluded from the analysis. Therefore, incorporating additional species into the study would enable a more comprehensive identification of genes involved in this pathological condition. However, the current lack of available data prevents such expansion. Furthermore, while data are available for other species, they primarily stem from clinical trials where the use of drugs could introduce potential biases.

Finally, due to the limited availability of publicly accessible data, we relied on datasets from heterogeneous tissues, which may introduce topographic variation biases that must be carefully considered.

Conclusion

Overall, a conserved response to ACL disruption has been observed across species, suggesting that similar molecular mechanisms are affected in different species despite variations in the experimental conditions. We found that this conserved response is activated by the up- and down-regulation of genes and pathways across species, which play a role in various biological processes, such as cartilage metabolism, bone mineralization, mitosis, and lipid metabolism. Furthermore, several genes and pathways identified herein have already been linked to ACL rupture and osteoarthritis. The cross-species similarities highlight that ACL trauma involves conserved biological processes, despite differences in experimental conditions (spontaneous or surgically induced rupture, sampled tissue, and timing after the injury) and the phylogenetic distance among the included species. The evidence that gene expression changes are widely correlated between humans and the other three species after the injury (Figs. 1 and 2B) reinforces the value of dogs, mice, and rabbits as effective translational animal models for studying human diseases, particularly anterior cruciate ligament disruption.

Supplementary Information

The online version contains supplementary material available at <https://doi.org/10.1186/s12864-025-11702-x>.

Supplementary Material 1

Supplementary Material 2

Author contributions

LB: Methodology, Software, Formal analysis, Investigation, Data curation, Writing - Original draft, Visualization; SP: Conceptualization, Writing- Review & Editing; YL: Investigation; JH: Writing- Review & Editing, Supervision; LP: Writing- Review & Editing, Supervision; VN: Conceptualization, Resources, Writing- Review & Editing, Supervision, Project Administration.

Funding

No fundings.

Data availability

The samples generated by previous projects and used in this study are available in the NCBI Sequence Read Archive (SRA) [PRJNA694471, PRJNA879078, PRJNA448594, PRJNA1134075, PRJEB43144, PRJNA751479].

Declarations

Ethics approval and consent to participate

Not applicable.

Consent for publication

Not applicable.

Competing interests

The authors declare no competing interests.

Received: 10 March 2025 / Accepted: 12 May 2025

Published online: 23 May 2025

References

1. Siegel L, Vandenakker-Albanese C, Siegel D. Anterior cruciate ligament injuries: anatomy, physiology, biomechanics, and management. *Clin J Sport Med*. 2012;22:349–55.
2. Whittaker JL, Losciale JM, Juhl CB, Thorlund JB, Lundberg M, Truong LK, et al. Risk factors for knee osteoarthritis after traumatic knee injury: a systematic review and meta-analysis of randomised controlled trials and cohort studies for the OPTIKNEE consensus. *Br J Sports Med*. 2022;56:1406–21.
3. Wang L-J, Zeng N, Yan Z-P, Li J-T, Ni G-X. Post-traumatic osteoarthritis following ACL injury. *Arthritis Res Ther*. 2020;22:57.
4. Giorgino R, Albano D, Fusco S, Peretti GM, Mangiavini L, Messina C. Knee osteoarthritis: epidemiology, pathogenesis, and mesenchymal stem cells: what else is new?? An update. *Int J Mol Sci*. 2023;24:6405.
5. Sutton KM, Bullock JM. Anterior cruciate ligament rupture: differences between males and females. *J Am Acad Orthop Surg*. 2013;21:41–50.
6. Alsayed HN, Alkhateeb MA, Aldossary AA, Houbani KM, Aljamaan YM, Alrashidi YA. Risk of anterior cruciate ligament injury in population with elevated body mass index. *Med Glas (Zenica)*. 2023;20.
7. Sun Z, Cieszczyk P, Humińska-Lisowska K, Michałowska-Sawczyn M, Yue S. Genetic determinants of the anterior cruciate ligament rupture in sport: an Up-to-Date systematic review. *J Hum Kinet*. 2023;87:105–17.
8. Napolioni V, Bianconi F, Potenza R, Carpi FM, Ludovini V, Piccoliini M, et al. Genome-wide expression of the residual lung reacting to experimental pneumonectomy. *BMC Genomics*. 2021;22:881.
9. Pallotti S, Piras IS, Marchegiani A, Cerquetella M, Napolioni V. Dog-human translational genomics: state of the Art and genomic resources. *J Appl Genet*. 2022;63:703–16.
10. Yang R, Xu T, Zhang L, Ge M, Yan L, Li J, et al. A single-cell atlas depicting the cellular and molecular features in human anterior cruciate ligament degeneration: A single cell combined Spatial transcriptomics study. *Elife*. 2023;12:e85700.
11. Bergman RF, Lammlin L, Junginger L, Farrell E, Goldman S, Darcy R, et al. Sexual dimorphism of the synovial transcriptome underpins greater PTOA disease severity in male mice following joint injury. *Osteoarthritis Cartilage*. 2024;32:1060–73.

12. Gu H, Chen S, Zhang M, Wen Y, Li B. Differences in the expression profiles of lncRNAs and mRNAs in partially injured anterior cruciate ligament and medial collateral ligament of rabbits. *PeerJ*. 2022;10:e12781.
13. Baker LA, Momen M, McNally R, Berres ME, Binversie EE, Sample SJ, et al. Biologically enhanced Genome-Wide association study provides further evidence for candidate loci and discovers novel loci that influence risk of anterior cruciate ligament rupture in a dog model. *Front Genet*. 2021;12:593515.
14. Sayers EW, Beck J, Bolton EE, Brister JR, Chan J, Connor R, et al. Database resources of the National center for biotechnology information in 2025. *Nucleic Acids Res*. 2025;53:D20–9.
15. Xiao X, Yang X, Ren S, Meng C, Yang Z. Construction and analysis of a lncRNA-miRNA-mRNA competing endogenous RNA network from inflamed and normal synovial tissues after anterior cruciate ligament and/or meniscus injuries. *Front Genet*. 2022;13:983020.
16. Sebastian A, Chang JC, Mendez ME, Murugesh DK, Hatsell S, Economides AN, et al. Comparative transcriptomics identifies novel genes and pathways involved in Post-Traumatic osteoarthritis development and progression. *Int J Mol Sci*. 2018;19:2657.
17. Andrews S, Babraham Bioinformatics - FastQC A Quality Control tool for High Throughput Sequence Data. 2010. <https://www.bioinformatics.babraham.ac.uk/projects/fastqc/>. Accessed 25 Feb 2025.
18. Bolger AM, Lohse M, Usadel B. Trimmomatic: a flexible trimmer for illumina sequence data. *Bioinformatics*. 2014;30:2114–20.
19. Dobin A, Davis CA, Schlesinger F, Drenkow J, Zaleski C, Jha S, et al. STAR: ultrafast universal RNA-seq aligner. *Bioinformatics*. 2013;29:15–21.
20. Liao Y, Smyth GK, Shi W. FeatureCounts: an efficient general purpose program for assigning sequence reads to genomic features. *Bioinformatics*. 2014;30:923–30.
21. Wickham H. ggplot2: elegant graphics for data analysis. New York: Springer; 2016.
22. Love MI, Huber W, Anders S. Moderated Estimation of fold change and dispersion for RNA-seq data with DESeq2. *Genome Biol*. 2014;15:550.
23. Hu Y, Flockhart I, Vinayagam A, Bergwitz C, Berger B, Perrimon N, et al. An integrative approach to ortholog prediction for disease-focused and other functional studies. *BMC Bioinformatics*. 2011;12:357.
24. Schilder B, Skene N. orthogene: an R package for easy mapping of orthologous genes across hundreds of species. *Bioconductor*. 2022. <http://bioconductor.org/packages/orthogene/>. Accessed 25 Feb 2025.
25. Mercatelli D, Lopez-Garcia G, Giorgi FM. Corto: a lightweight R package for gene network inference and master regulator analysis. *Bioinformatics*. 2020;36:3916–7.
26. Ashburner M, Ball CA, Blake JA, Botstein D, Butler H, Cherry JM, et al. Gene ontology: tool for the unification of biology. The gene ontology consortium. *Nat Genet*. 2000;25:25–9.
27. Gene Ontology Consortium, Aleksander SA, Balhoff J, Carbon S, Cherry JM, Drabkin HJ, et al. The gene ontology knowledgebase in 2023. *Genetics*. 2023;224:iyad031.
28. Kanehisa M, Goto S. KEGG: Kyoto encyclopedia of genes and genomes. *Nucleic Acids Res*. 2000;28:27–30.
29. Kanehisa M, Furumichi M, Sato Y, Matsuura Y, Ishiguro-Watanabe M. KEGG: biological systems database as a model of the real world. *Nucleic Acids Res*. 2025;53:D672–7.
30. Agrawal A, Balci H, Hanspers K, Coort SL, Martens M, Slenter DN, et al. WikiPathways 2024: next generation pathway database. *Nucleic Acids Res*. 2024;52:D679–89.
31. Liberzon A, Birger C, Thorvaldsdóttir H, Ghandi M, Mesirov JP, Tamayo P. The molecular signatures database (MSigDB) hallmark gene set collection. *Cell Syst*. 2015;1:417–25.
32. Dolgalev I. msigdb: MSigDB Gene Sets for Multiple Organisms in a Tidy Data Format. 2025. <https://igordot.github.io/msigdb/>
33. Subramanian A, Tamayo P, Mootha VK, Mukherjee S, Ebert BL, Gillette MA, et al. Gene set enrichment analysis: a knowledge-based approach for interpreting genome-wide expression profiles. *Proc Natl Acad Sci U S A*. 2005;102:15545–50.
34. Korotkevich G, Sukhov V, Sergushichev A. Fast gene set enrichment analysis. *Bioconductor*. 2019. <http://bioconductor.org/packages/fgsea/>. Accessed 25 Feb 2025.
35. Yu G, Wang L-G, Han Y, He Q-Y. ClusterProfiler: an R package for comparing biological themes among gene clusters. *OMICS*. 2012;16:284–7.
36. Proffen BL, McElfresh M, Fleming BC, Murray MM. A comparative anatomical study of the human knee and six animal species. *Knee*. 2012;19:493–9.
37. Bascuñán AL, Biedrzycki A, Banks SA, Lewis DD, Kim SE. Large animal models for anterior cruciate ligament research. *Front Vet Sci*. 2019;6:292.
38. Binversie EE, Walczak BE, Cone SG, Baker LA, Scerpella TA, Muir P. Canine ACL rupture: a spontaneous large animal model of human ACL rupture. *BMC Musculoskelet Disord*. 2022;23:116.
39. Butt U, Khan ZA, Zahir N, Khan Z, Vuletic F, Shah I, et al. Histological and cellular evaluation of anterior cruciate ligament. *Knee*. 2020;27:1510–8.
40. Donnenfeld JI, Fleming BC, Proffen BL, Podury A, Murray MM. Microscopic and transcriptomic changes in Porcine synovium one year following disruption of the anterior cruciate ligament. *Osteoarthritis Cartilage*. 2023;31:1554–66.
41. Caso E, Maestro A, Sabiers CC, Godino M, Caracul Z, Pons J, et al. Whole-exome sequencing analysis in twin sibling males with an anterior cruciate ligament rupture. *Injury*. 2016;47(Suppl 3):S41–50.
42. Satz-Jacobowitz B, Hubmacher D. The quest for substrates and binding partners: A critical barrier for Understanding the role of ADAMTS proteases in musculoskeletal development and disease. *Dev Dyn*. 2021;250:8–26.
43. Yang S, Zhou X, Jia Z, Zhang M, Yuan M, Zhou Y, et al. Epigenetic regulatory mechanism of ADAMTS12 expression in osteoarthritis. *Mol Med*. 2023;29:86.
44. Li Z, Zhang S, Mao G, Xu Y, Kang Y, Zheng L et al. Identification of anterior cruciate ligament fibroblasts and their contribution to knee osteoarthritis progression using single-cell analyses. *Int Immunopharmacol*. 2023;125 Pt A:111109.
45. Liang F, Peng L, Ma Y-G, Hu W, Zhang W-B, Deng M, et al. Bioinformatics analysis and experimental validation of differentially expressed genes in mouse articular chondrocytes treated with IL-1 β using microarray data. *Exp Ther Med*. 2022;23:6.
46. Shimizu H, Shimoda M, Mochizuki S, Miyamae Y, Abe H, Chijiwa M, et al. Hyaluronan-Binding protein involved in hyaluronan depolymerization is Up-Regulated and involved in hyaluronan degradation in human Osteoarthritic cartilage. *Am J Pathol*. 2018;188:2109–19.
47. Spataro S, Guerra C, Cavalli A, Sgrignani J, Sleeman J, Poulain L, et al. CEMIP (HYBID, KIAA1199): structure, function and expression in health and disease. *FEBS J*. 2023;290:3946–62.
48. Zhang B, Du Y, He Y, Liu Y, Zhang G, Yang C, et al. INT-HA induces M2-like macrophage differentiation of human monocytes via TLR4-miR-935 pathway. *Cancer Immunol Immunother*. 2019;68:189–200.
49. Shiozawa J, de Vega S, Cilek MZ, Yoshinaga C, Nakamura T, Kasamatsu S, et al. Implication of HYBID (Hyaluronan-Binding protein involved in hyaluronan Depolymerization) in hyaluronan degradation by synovial fibroblasts in patients with knee osteoarthritis. *Am J Pathol*. 2020;190:1046–58.
50. Shiozawa J, de Vega S, Yoshinaga C, Ji X, Negishi Y, Momoeda M, et al. Expression and regulation of recently discovered hyaluronidases, HYBID and TMEM2, in chondrocytes from knee Osteoarthritic cartilage. *Sci Rep*. 2022;12:17242.
51. Deroyer C, Charlier E, Neuville S, Malaise O, Gillet P, Kurth W, et al. CEMIP (KIAA1199) induces a fibrosis-like process in Osteoarthritic chondrocytes. *Cell Death Dis*. 2019;10:103.
52. Conde J, Scotece M, Abella V, Gómez R, López V, Villar R, et al. Identification of novel adipokines in the joint. Differential expression in healthy and osteoarthritis tissues. *PLoS ONE*. 2015;10:e0123601.
53. Ikuta K, Hayashi S, Kikuchi K, Fujita M, Anjiki K, Onoi Y, et al. Krüppel-like factor 15 deficiency exacerbates osteoarthritis through reduced expression of peroxisome proliferator-activated receptor gamma signaling in mice. *Osteoarthritis Cartilage*. 2024;32:28–40.
54. Fan A, Wu G, Wang J, Lu L, Wang J, Wei H, et al. Inhibition of fibroblast activation protein ameliorates cartilage matrix degradation and osteoarthritis progression. *Bone Res*. 2023;11:3.
55. McGregor NE, Poulton IJ, Walker EC, Pompolo S, Quinn JMW, Martin TJ, et al. Ciliary neurotrophic factor inhibits bone formation and plays a sex-specific role in bone growth and remodeling. *Calcif Tissue Int*. 2010;86:261–70.
56. Zhao M, Dong J, Liao Y, Lu G, Pan W, Zhou H, et al. MicroRNA miR-18a-3p promotes osteoporosis and possibly contributes to spinal fracture by inhibiting the glutamate AMPA receptor subunit 1 gene (GRIA1). *Bioengineered*. 2022;13:370–82.
57. Cai Z, Liu W, Chen K, Wang P, Xie Z, Li J, et al. Aberrantly expressed lncRNAs and mRNAs of osteogenically differentiated mesenchymal stem cells in ossification of the posterior longitudinal ligament. *Front Genet*. 2020;11:896.
58. den Hollander W, Pulyakhina I, Boer C, Bomer N, van der Breggen R, Arindart W, et al. Annotating transcriptional effects of genetic variants in Disease-Relevant tissue: Transcriptome-Wide allelic imbalance in Osteoarthritic cartilage. *Arthritis Rheumatol*. 2019;71:561–70.

59. Wei T, Kulkarni NH, Zeng QQ, Helvering LM, Lin X, Lawrence F, et al. Analysis of early changes in the articular cartilage transcriptome in the rat meniscal tear model of osteoarthritis: pathway comparisons with the rat anterior cruciate transection model and with human Osteoarthritic cartilage. *Osteoarthritis Cartilage*. 2010;18:992–1000.
60. Ohsawa N, Koebis M, Mitsuhashi H, Nishino I, Ishiura S. ABLIM1 splicing is abnormal in skeletal muscle of patients with DM1 and regulated by MBNL, CELF and PTBP1. *Genes Cells*. 2015;20:121–34.
61. Little D, Thompson JW, Dubois LG, Ruch DS, Moseley MA, Guilak F. Proteomic differences between male and female anterior cruciate ligament and patellar tendon. *PLoS ONE*. 2014;9:e96526.
62. Liu YM, Yip SK, Wong WY, Smith DI, Wong YF. Gene expression profiling of Cardinal ligament in Hong Kong Chinese women with pelvic organ prolapse. *Neurourol Urodyn*. 2005;24:13.
63. Shen Y, White E. p53-dependent apoptosis pathways. *Adv Cancer Res*. 2001;82:55–84.
64. Zhu X, Yang S, Lin W, Wang L, Ying J, Ding Y, et al. Roles of cell cycle regulators Cyclin D1, CDK4, and p53 in knee osteoarthritis. *Genet Test Mol Biomarkers*. 2016;20:529–34.
65. Ashraf S, Cha B-H, Kim J-S, Ahn J, Han I, Park H, et al. Regulation of senescence associated signaling mechanisms in chondrocytes for cartilage tissue regeneration. *Osteoarthritis Cartilage*. 2016;24:196–205.
66. Li W, Xiong Y, Chen W, Wu L. Wnt/ β -catenin signaling May induce senescence of chondrocytes in osteoarthritis. *Exp Ther Med*. 2020;20:2631–8.
67. van Meer BL, Waarsing JH, van Eijnsden WA, Meuffels DE, van Arkel ERA, Verhaar J et al. a. N. Bone mineral density changes in the knee following anterior cruciate ligament rupture. *Osteoarthritis Cartilage*. 2014;22:154–61.
68. Patton DM, Ochocki DN, Martin CT, Casden M, Jepsen KJ, Ashton-Miller JA, et al. State of the mineralized tissue comprising the femoral ACL enthesis in young women with an ACL failure. *J Orthop Res*. 2022;40:826–37.
69. Beaulieu ML, Wang Y, Schlecht SH, Ashton-Miller JA, Wojtyś EM. Mineralized tissue loss at the femoral ACL enthesis in young male ACL-injured patients. *J Exp Orthop*. 2025;12:e70106.
70. Ahn T, Loflin BE, Nguyen NB, Miller CK, Colglazier KA, Wojtyś EM, et al. Acute bone loss and infrapatellar fat pad fibrosis in the knee after an in vivo ACL injury in adolescent mice. *Am J Sports Med*. 2023;51:2342–56.
71. Yao Q, Wu X, Tao C, Gong W, Chen M, Qu M, et al. Osteoarthritis: pathogenic signaling pathways and therapeutic targets. *Signal Transduct Target Ther*. 2023;8:56.
72. Aspden RM, Scheven BA, Hutchison JD. Osteoarthritis as a systemic disorder including stromal cell differentiation and lipid metabolism. *Lancet*. 2001;357:1118–20.
73. Tufts LS, Shet K, Liang F, Majumdar S, Li X. Quantification of bone marrow water and lipid composition in anterior cruciate ligament-injured and Osteoarthritic knees using three-dimensional magnetic resonance spectroscopic imaging. *Magn Reson Imaging*. 2016;34:632–7.
74. Loeff M, Schoones JW, Kloppenburg M, Ioan-Facsinay A. Fatty acids and osteoarthritis: different types, different effects. *Joint Bone Spine*. 2019;86:451–8.
75. Abshirini M, Ilesanmi-Oyelere BL, Kruger MC. Potential modulatory mechanisms of action by long-chain polyunsaturated fatty acids on bone cell and chondrocyte metabolism. *Prog Lipid Res*. 2021;83:101113.
76. Nakanishi A, Tsukamoto I. n-3 polyunsaturated fatty acids stimulate osteoclastogenesis through PPAR γ -mediated enhancement of c-Fos expression, and suppress osteoclastogenesis through PPAR γ -dependent inhibition of NF κ B activation. *J Nutr Biochem*. 2015;26:1317–27.

Publisher's note

Springer Nature remains neutral with regard to jurisdictional claims in published maps and institutional affiliations.